Analyses of Resected Human Brain Metastases of Breast Cancer Reveal the Association between Up-Regulation of Hexokinase 2 and Poor Prognosis

Diane Palmieri,[1] Daniel Fitzgerald,[1] S. Martin Shreeve,[1] Emily Hua,[1] Julie L. Bronder,[1] Robert J. Weil,[5] Sean Davis,[6] Andreas M. Stark,[6] Maria J. Merino,[3] Raffael Kurek,[7] H. Maximilian Mehdorn,[2] Gary Davis,[8] Seth M. Steinberg,[4] Paul S. Meltzer,[2] Kenneth Aldape,[9] and Patricia S. Steeg[1]

[1]Women's Cancers Section, Laboratory of Molecular Pharmacology, [2]Genetics Branch, [3]Surgical Pathology Section, Laboratory of Pathology, and [4]Biostatistics and Data Management Section, Center for Cancer Research, National Cancer Institute, Bethesda, Maryland; [5]Brain Tumor Institute, Cleveland Clinic Foundation, Cleveland, Ohio; [6]University of Schleswig-Holstein Medical Center, Kiel, Germany; [7]University of Tuebingen, Tuebingen, Germany; [8]Sigma-Aldrich Biotechnology, St. Louis, Missouri; and [9]Department of Neurosurgery, M. D. Anderson Cancer Center, Houston, Texas

Abstract

Brain metastases of breast cancer seem to be increasing in incidence as systemic therapy improves. Metastatic disease in the brain is associated with high morbidity and mortality. We present the first gene expression analysis of laser-captured epithelial cells from resected human brain metastases of breast cancer compared with unlinked primary breast tumors. The tumors were matched for histology, tumor-node-metastasis stage, and hormone receptor status. Most differentially expressed genes were down-regulated in the brain metastases, which included, surprisingly, many genes associated with metastasis. Quantitative real-time PCR analysis confirmed statistically significant differences or strong trends in the expression of six genes: *BMP1, PEDF, LAMγ3, SIAH, STHMN3*, and *TSPD2*. Hexokinase 2 (HK2) was also of interest because of its increased expression in brain metastases. HK2 is important in glucose metabolism and apoptosis. In agreement with our microarray results, HK2 levels (both mRNA and protein) were elevated in a brain metastatic derivative (231-BR) of the human breast carcinoma cell line MDA-MB-231 relative to the parental cell line (231-P) *in vitro*. Knockdown of HK2 expression in 231-BR cells using short hairpin RNA reduced cell proliferation when cultures were maintained in glucose-limiting conditions. Finally, HK2 expression was analyzed in a cohort of 123 resected brain metastases of breast cancer. High HK2 expression was significantly associated with poor patient survival after craniotomy ($P = 0.028$). The data suggest that HK2 overexpression is associated with metastasis to the brain in breast cancer and it may be a therapeutic target. (Mol Cancer Res 2009;7(9):1438–45)

Introduction

Metastasis to the central nervous system (brain) is a contributor to breast cancer patient morbidity and mortality. Traditionally, brain metastases were diagnosed in ~15% of metastatic breast cancer patients late in the course of their disease and only palliative treatment was given. Improvements in breast cancer treatment have increased the number of patients with systemic responses and lengthened survival; however, brain metastases have also increased as a "sanctuary" site (reviewed in refs. 1, 2). This is best quantified in the Her-2^+ subpopulation of breast cancers, where studies document that 25% to 40% of metastatic patients now develop brain metastases, often as the first site of relapse (reviewed in ref. 3). Other risk factors for brain metastases include "triple-negative" or basal primary tumors, systemic metastases, and young patient age (4-11). To understand the molecular events that underlie brain metastases, we initiated a gene expression profiling experiment using resected brain metastases of breast cancer.

Among the trends in gene expression, the overexpression of hexokinase 2 (HK2) was observed in brain metastases. HK2 is one of four members of the hexokinase family. The isoenzymes (HK1, HK2, HK3, and glucokinase) are structurally similar; however, only HK1 and HK2 are functionally similar. HK2, but not HK1, is overexpressed in several cancer types compared with normal tissues; among primary tumors, high HK2 confers a poor prognosis (12-15). Ample evidence suggests that HK2 biochemical pathways are heightened in cancer and may constitute a potential therapeutic target. HK2 plays a key step early in glycolysis, phosphorylating glucose to produce glucose-6-phosphate. In some cell types, HK2 binds to the mitochondrial membrane to obtain ATP exported from oxidative phosphorylation. The K_m for Mg-ATP bound to the mitochondrial membrane

Received 5/27/09; revised 7/10/09; accepted 7/16/09; published OnlineFirst 9/1/09.
Grant support: National Cancer Institute Intramural program and Department of Defense Breast Cancer Research Program grant W81XWH-062-0033.
The costs of publication of this article were defrayed in part by the payment of page charges. This article must therefore be hereby marked *advertisement* in accordance with 18 U.S.C. Section 1734 solely to indicate this fact.
Note: Current address for S.M. Shreeve: Pfizer Global Research and Development, Pfizer, Inc., La Jolla, California. Current address for J.L. Bronder: Cancer Center Training Branch, National Cancer Institute, Rockville, Maryland. Current address for R. Kurek: ImClone Systems International GmbH, Heidelberg, Germany.
Requests for reprints: Patricia S. Steeg, Women's Cancers Section, Laboratory of Molecular Pharmacology, Center for Cancer Research, National Cancer Institute, Building 37, Room 1122, 9000 Rockville Pike, Bethesda, MD 20892-7322. Phone: 301-402-2732; Fax: 301-402-8910. E-mail: steegp@mail.nih.gov

doi:10.1158/1541-7786.MCR-09-0234

Table 1. Histologic Characteristics of Microarray Specimens

Specimen	Site	TNM*	ER	Her-2	Histology
4-11-1	BM	T1 N0	Neg.	Amp.	Ductal
4-11-2	BM	T2 N1 M0	Pos.	wt	Ductal
4-11-3	BM	T3 N2	Pos.	wt	Lobular
4-11-4	BM	T3 N1 M0	Neg.	wt	Inflammatory
4-11-5	BM	T3 N2 M0	Pos.	Amp.	Ductal
4-11-6	BM	T2 N1 M0	Neg.	Amp.	Ductal
4-11-7	BM	T2 N1 M0	Neg.	Amp.	Ductal
4-11-8	BM	T1 N0	Pos.	wt	Ductal
4-11-9	P	T2 N1	Neg.	wt	Ductal
4-11-10	P	T1 N0	Pos.	Amp.	Ductal
4-11-11	P	T1	Pos.	wt	Ductal
4-11-12	P	T2 N0	Neg.	wt	Ductal
4-11-13	P	T2 N1	Neg.	wt	Lobular
4-11-14	P	T2 N1	Neg.	wt	Ductal
4-11-15	P	T1	Pos.	wt	Ductal
4-11-16	P	T2	Pos.	wt	Ductal
4-11-17	P	T3 N2 Mx	Neg.	wt	Ductal

Abbreviations: BM, brain metastasis; P, primary tumor; TNM, tumor-node-metastasis; Pos., positive by immunohistochemistry; Neg., negative; Amp, amplified by fluorescence *in situ* hybridization; wt, wild-type DNA level.
*Histology of brain metastases based on patient's primary tumor.

is approximately five times lower than that of free Mg-ATP (16). This efficient coupling of ATP from oxidative phosphorylation to the rate-limiting step of glycolysis may contribute to the Warburg effect, where tumor cells use glycolysis even in the presence of oxygen (16, 17). Not only does HK2 participate in bioenergetics, but its association with mitochondria has also been reported to prevent apoptosis (reviewed in ref. 18). HK2 binds to the voltage-dependent anion channel (VDAC) on the mitochondrial membrane. In turn, the VDAC/HK2 complex forms part of the permeability transition pore together with cyclophilin D and adenine nucleotide translocase (17, 19). How HK2 physically blocks apoptosis is still under investigation. One model suggests that the proapoptotic protein Bax also physically binds VDAC (in the absence of HK2) to promote cytochrome *c* release. Alternatively, HK2 may modulate binding of the antiapoptotic protein Bcl-Xl to VDAC, with consequences for its downstream partnering with Bak and Bax (reviewed in ref. 20). HK2 expression may also influence [^{18}F]2-fluoro-2-deoxy-D-glucose uptake in tumors, thus affecting positron emission tomography imaging for diagnosis and staging (13, 21, 22).

This study presents the first analysis of differentially expressed genes between resected brain metastases and primary breast carcinomas. A trend of elevated HK2 expression in brain metastases is shown. In a brain metastasis cell line model, knockdown of HK2 expression reduced cellular viability under conditions of limited glucose availability. Finally, the relevance of differential HK2 expression is shown by the association of high HK2 expression in brain metastases with reduced patient survival.

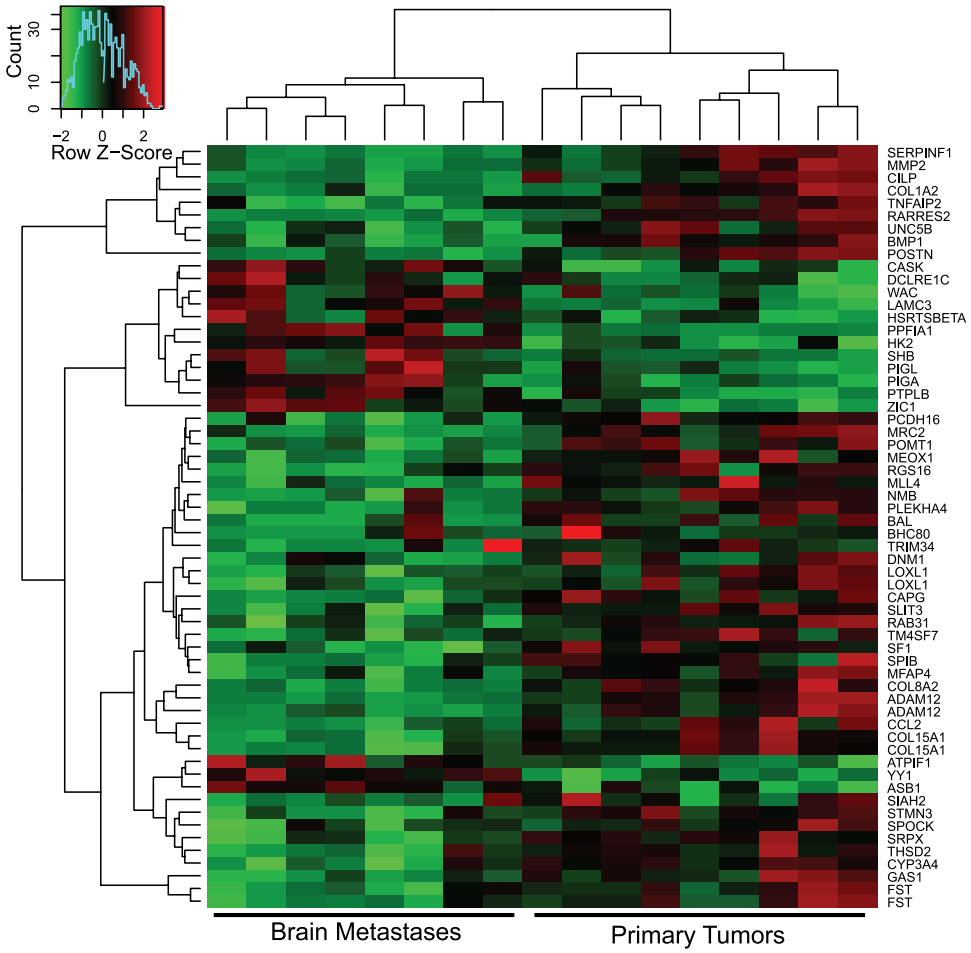

FIGURE 1. Microarray analysis of resected human brain metastases of breast cancer and unlinked primary breast tumors. Epithelial cells were procured by LCM from brain metastases and primary tumors. Extracted and amplified RNAs were converted to Cy-dUTP–labeled cDNA and hybridized to a 30K cDNA microarray. The control hybridization consisted of a mixture of RNAs from six human breast cancer cell lines, similarly processed. Supervised clustering of the data is shown where each sample is identified as a brain metastasis (*left*) or a primary tumor (*right*).

Table 2. Q-PCR Validation of Differentially Expressed Genes

Gene	Trend on microarray	Mean ± SE*		$P^{\dagger}$
		Brain metastasis	Primary tumor	
BHC80	Down in BM	22.5 ± 4.9	63 ± 17.2	0.22
BMP1	Down in BM	2.8 ± 0.5	7.1 ± 1.4	0.01
HK2	Up in BM	0.9 ± 0.2	0.6 ± 0.1	0.13
LAMγ3	Up in BM	0.7 ± 0.2	0.3 ± 0.1	0.05
LOXL1	Down in BM	3.8 ± 0.6	9.0 ± 2.6	0.14
PEDF	Down in BM	5.4 ± 3.1	76.0 ± 36.5	0.001
SIAH	Down in BM	1.0 ± 0.3	6.6 ± 2.8	0.00011
SLIT3	Down in BM	1.1 ± 0.3	2.4 ± 0.7	0.26
STHMN3	Down in BM	0.6 ± 0.2	1.9 ± 0.6	0.0087
TSPD2	Down in BM	0.1 ± 0.1	2.7 ± 0.8	0.00014

Abbreviation: BM, brain metastasis.
*Adjusted for glyceraldehyde-3-phosphate dehydrogenase levels.
†By exact two-tailed Wilcoxon rank sum test.

Results

Microarray Analysis of Resected Brain Metastases and Unlinked Primary Breast Tumors

To identify potential molecular therapeutic targets for brain metastases of breast cancer, resected human brain metastases and unlinked primary tumors were subjected to a microarray analysis. Tissues were sectioned and epithelial cells were procured by laser capture microdissection (LCM). Of 16 flash-frozen brain metastases, 8 produced RNA of sufficient quality for hybridization, as did 9 of 20 primary breast tumors. Table 1 lists the characteristics of the tumors used. Most of the histologic indicators were well balanced between the primary tumors and brain metastases. Tumors varied from T1 to T3 and N0 to N2 in both cohorts. Four of eight brain metastases and four of nine primary tumors were estrogen receptor (ER) positive. Most of the specimens were ductal in histology, with a lobular carcinoma in each cohort and a single brain metastasis from an inflammatory primary tumor. Her-2 amplification was overrepresented in the brain metastases cohort (four of eight) compared with the primary tumors (one of nine).

A heat map displays the top 60 differentially expressed genes between the brain metastases and the primary tumors based on supervised hierarchical clustering and elimination of expression signatures associated with common breast cancer pathways, such as ER and Her-2 (Fig. 1). The majority of differentially regulated genes were down-regulated in the brain metastases. Notably, metastasis-associated genes were also down-regulated in the brain metastases, including genes involved in extracellular matrix function (*MMP2, COL1A2, LOXL1, MFAP4, COL8A2, ADAM12, COL15A1*, and *THSD2*), cell adhesion (*PCDH16* and *TM4SF7*), and motility (*UNC5B, CAPG, CCL2*, and *STMN3*). Up-regulated genes included phosphatases (*PPFIA1* and *PTPLB*), phosphoinositide glycan anchor biosynthetic proteins that glycosylphosphatidylinositol anchor proteins to membranes (*PIGL* and *PIGA*), and signaling proteins (*CASK* and *SHB*). The only extracellular matrix gene up-regulated in the brain metastases was *LAMγ3*, a component of laminin 12.

Because of the small number of specimens profiled and the rarity of resected brain metastases suitable for molecular analysis, validation experiments used four of the initially profiled specimens, in an attempt to repeat the gene expression trends observed on the microarray, supplemented with eight independent samples each of unlinked brain metastases and primary tumors. Quantitative real-time PCR (Q-PCR) was done on amplified cDNA from laser capture microdissected epithelial cells. Table 2 lists the expression levels of nine genes from the microarray analysis. Significant differences or strong trends in the expression of several down-regulated genes were observed, including *BMP1*, which regulates cartilage formation ($P = 0.01$), *SIAH*, seven in abstentia homologue 1 ($P = 0.001$), *STHMN3*, stathmin-like 3 ($P = 0.009$), and *TSPD2*, a thrombospondin derivative ($P = 0.0001$). Two genes were up-regulated in brain metastases in the microarray analysis and the validation cohort: *LAMγ3*, a component of laminin 12 ($P = 0.05$), and *HK2* ($P = 0.13$). Because of the potential contributions of HK2 to tumor cell bioenergetics, growth, and apoptosis, as well as the potential of HK2 to be pharmacologically inhibited, functional studies of altered HK2 expression were initiated.

Knockdown of HK2 Impairs Proliferation under Glucose-Limiting Culture Conditions

The human breast carcinoma cell line MDA-MB-231 was selected through six rounds of *in vivo* passage for a brain metastastic subline (231-BR; refs. 23, 24). Several of the validated gene expression trends noted above between brain metastases

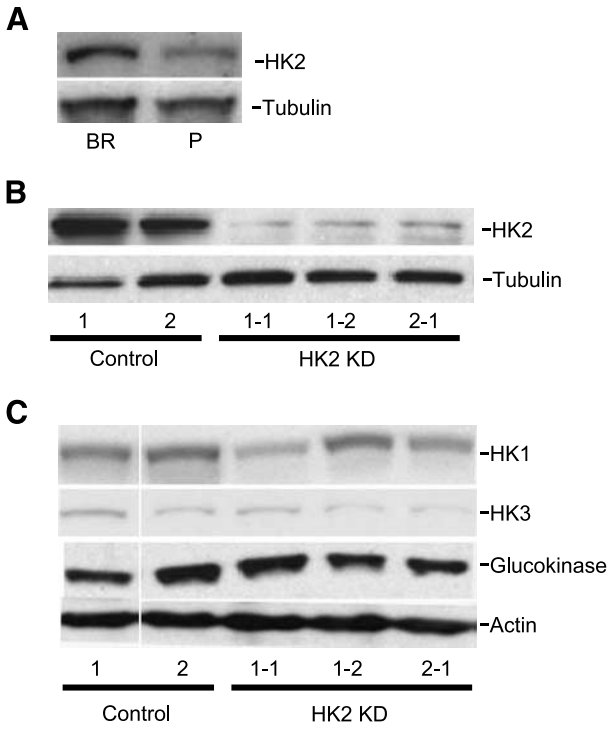

FIGURE 2. Western blot analysis of HK2 expression in the 231-BR model system. **A.** HK2 protein levels in parental MDA-MB-231 human breast cancer cells (*P*) and a brain metastatic derivative (*BR*). Tubulin is shown as a loading control. **B.** Knockdown of HK2 expression in 231-BR cells is shown, including two independent clones of HK2 shRNA 1 (*1-1* and *1-2*) and one clone of HK2 shRNA 2 (*2-1*). Two clonal lines expressing a control scrambled shRNA (*Controls 1* and *2*) are also shown. **C.** Expression levels of other hexokinase family members are not affected by HK2 knockdown. Protein levels for HK1, HK3, and glucokinase are shown for the clonal lines listed in **B**, with actin as a loading control.

and primary breast tumors were analyzed in the model system by comparing mRNA levels for a given gene between the parental MDA-MB-231 cell line and the 231-BR metastatic subclone. Of the six genes analyzed by Q-PCR, only HK2 exhibited the same trend as seen in the tumor cohort. The 231-BR cells had a 2-fold increase in HK2 mRNA levels (16.37; 95% confidence interval, 9.24-23.5) compared with parental MDA-MB-231 cells (7.98; 95% confidence interval, 4.82-11.13). Increased HK2 protein expression was also noted in the 231-BR line compared with parental MDA-MB-231 cells, further suggesting that increased HK2 expression is coincident with brain metastatic colonization (Fig. 2A). To test the functional consequences of altered HK2 expression, 231-BR cells were infected with a control short hairpin RNA (shRNA) or one of two HK2 shRNAs, and clones were isolated. Three independent clones expressing HK2 shRNA exhibited a 56% to 65% reduction in HK2 protein levels relative to control clones as determined by Western blot analysis (Fig. 2B). The shRNA constructs used to knock down HK2 are specific for this hexokinase family member as they did not seem to affect expression of the related isoenzyme family members, HK1, HK3, and glucokinase (Fig. 2C).

To determine if knockdown of HK2 altered cellular bioenergetics, intracellular ATP levels were determined over 4 days of culture (Fig. 3). Under standard culture conditions, intracellular ATP levels were unaffected by HK2 depletion (Fig. 3A), possibly the result of redundant activities of hexokinase homologue proteins, which are clearly present (Fig. 2C). However, under these culture conditions, glucose is in excess compared with physiologic conditions (4.5 g/L in standard growth medium compared with human serum levels of 7-11 mg/L). We therefore determined cellular ATP levels in limited glucose, 10% of standard culture conditions (Fig. 3B). ATP levels in the two control clones increased 5- to 6-fold over time; a smaller rate of ATP increase was observed in each of the HK2 knockdown clones (2- to 4-fold; $P < 0.005$ for each HK2 knockdown clone compared with the average of the controls and $P = 0.003$ for a comparison of the mean of the controls to the mean of the HK2 knockdown clones by one-way ANOVA). The amount of ATP is proportional to the number of viable cells, and as such, we confirmed these results using an MTT assay. No difference in viability was observed over 4 days of culture between the control and HK2 knockdown clones under standard culture conditions, whereas in limiting glucose concentrations the HK2 knockdown clones exhibited a pronounced decrease in viability compared with controls (data not shown). This observation was also confirmed by trypan blue exclusion cell counting. An attempt was made to assess the effect of low oxygen conditions on ATP levels/viability; no difference was observed between control and

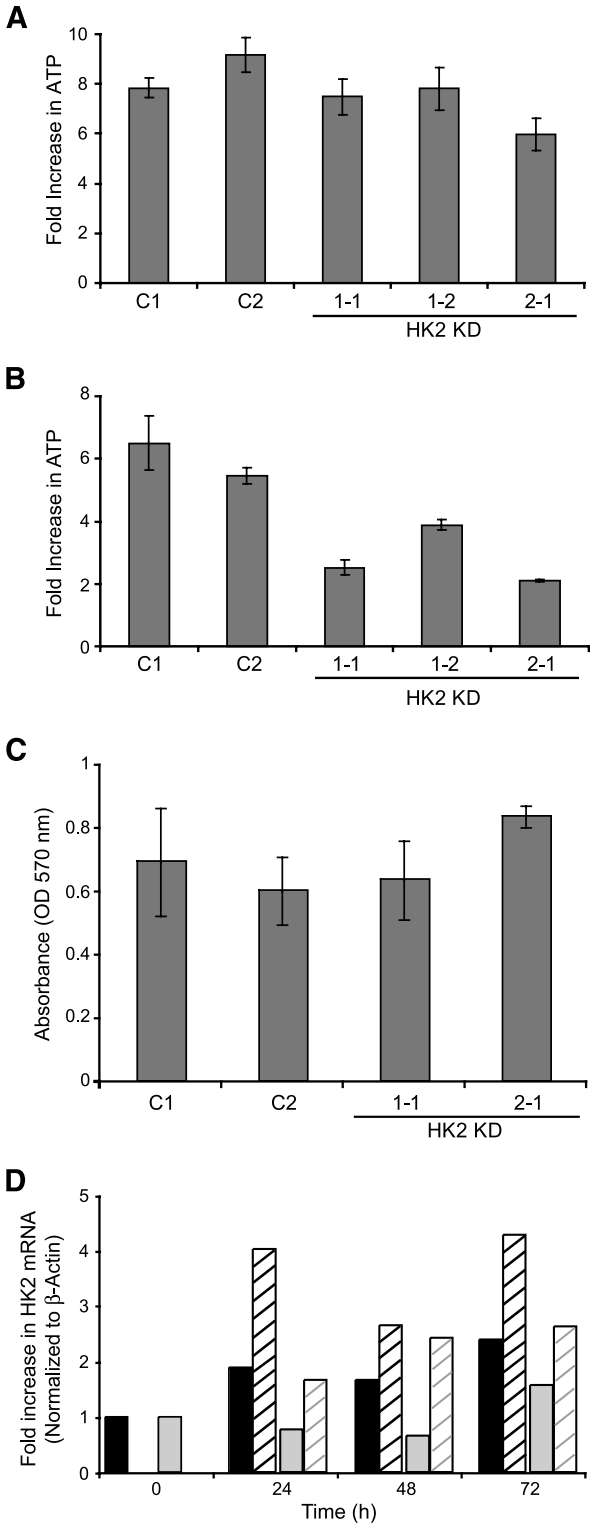

FIGURE 3. HK2 shRNA reduced cell viability, as measured by ATP concentration, of 231-BR cells *in vitro* under glucose-limiting conditions. **A.** The control shRNA and HK2 shRNA clones were grown in normal culture medium (high-glucose DMEM). **B.** The same clones were grown in medium diluted 10-fold into glucose-free DMEM for 4 d ($P < 0.0001$, one-way ANOVA). Cellular ATP levels were measured by CellTiter-Glo Luminescent Cell Viability Assay at 24 and 96 h of culture. Columns, mean fold increase for three experiments; bars, SD. **C.** Knockdown of HK2 expression did affect the viability of cells grown in hypoxic conditions. Columns, mean absorbance by MTT assay for three experiments; bars, SD. **D.** HK2 mRNA knockdown was overcome when cells were grown in hypoxic conditions. The fold increase in HK2 mRNA compared with each clone at $t = 0$ in normal growth conditions. HK2 mRNA was normalized to β-actin. Black columns, HK2 shRNA clone 1-1; gray columns, HK2 shRNA clone 2-1; hatched columns, clones grown in low oxygen conditions.

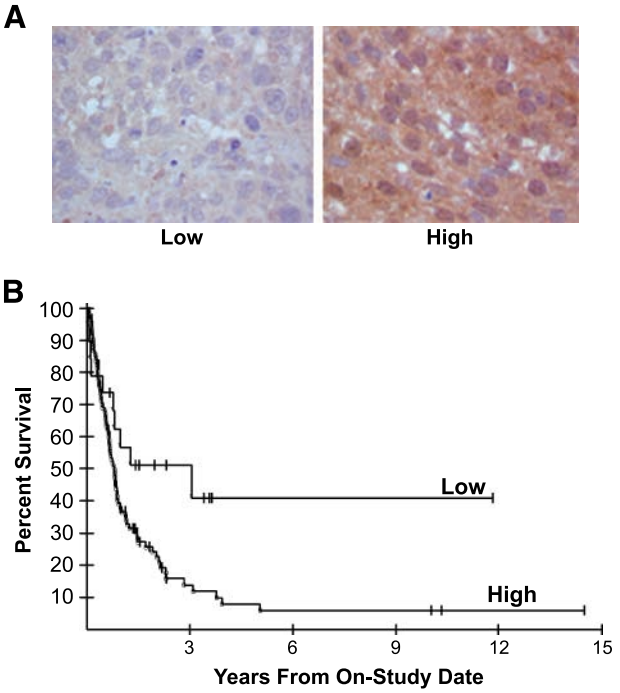

FIGURE 4. High HK2 expression in brain metastases predicts poor survival after craniotomy. **A.** The HK2 expression of 123 resected brain metastases of breast cancer was determined by immunohistochemistry; representative images of low and high levels of HK2 staining are shown. **B.** A Kaplan-Meier plot of patient survival after craniotomy shows reduced survival in the high HK2 subset ($P = 0.028$, two-tailed log-rank test).

HK2 knockdown clones when cultured in hypoxic conditions (Fig. 3C). Further analysis showed that HK2 knockdown was overcome under hypoxic conditions by an increase in HK2 mRNA levels (Fig. 3D).

The effect of decreased HK2 expression on drug-induced apoptosis was examined to identify a role for HK2 in cell death in the 231-BR cells. Control and HK2 knockdown clones of 231-BR cells were incubated for 48 hours in the presence or absence of 0.5 to 1.0 μmol/L of doxorubicin or 1 to 50 nmol/L of paclitaxel in standard growth conditions. Although both drugs showed a dose-dependent increase in apoptosis as measured by Cell Death Detection ELISA$^+$ for all cells, there was no consistent difference in the amount of apoptosis between the control and HK2 knockdown clones. Similar experiments were done using 5 Gy radiation as a relevant apoptosis inducer, and again, no significant difference was observed between control and knockdown clones (data not shown).

HK2 Protein Levels Are Associated with Survival after Resection

To further investigate HK2 as a potential molecular target for brain metastasis of breast cancer, we asked whether relative HK2 levels were associated with patient outcome after resection. Immunohistochemistry was done on a cohort of 123 resected brain metastases of breast cancer. The cohort of resected brain metastases was scored as having no, low, or high levels of HK2. Representative images of low and high HK2 staining levels are shown (Fig. 4A). Ninety-five of the 123 tumors (77%) expressed high levels of HK2 staining, and patient survival in this group was significantly reduced compared with the 19 of 123 (15%) patients with low tumor HK2 levels (Fig. 4B). The median survival for patients with high HK2 expression was 9.6 months, whereas that for patients with low HK2 expression tumors was 17.5 months ($P = 0.028$ for overall difference between the curves, by two-tailed log-rank test). With regard to conventional histologic markers, HK2 expression was not well associated with either Her-2 or ER expression ($P = 0.19$ and 0.26, respectively, two-tailed Fisher's exact test). Table 3 shows the results of a Cox proportional hazards model analysis of ER, Her-2, and HK2 staining data in this cohort. All three parameters were determined to be jointly statistically significant in this model. Furthermore, using a likelihood ratio test, HK2 expression provided a statistically significant increase in prognosis in the survival model beyond that of ER and Her-2 together ($P = 0.0033$). Thus, HK2 may be useful as a marker for prognosis in this population, if this finding were independently confirmed.

Discussion

Brain metastases are increasing in incidence in metastatic breast cancer patients and often occur when a patient is responding to treatment or has stable disease systemically (3, 25). Several factors suggest that this niche site may be molecularly distinct: We previously documented a prominent neuro-inflammatory response between brain metastatic breast cancer cells and activated host microglia and astrocytes both in the 231-BR mouse model and resected human brain metastases (26) and others have observed similar trends (27-29). These data suggest the existence of a unique tumor cell-microenvironmental interaction. Second, the brain is known as a sanctuary site (reviewed in ref. 30). Although the blood-brain barrier (BBB) severely restricts access of drugs and cytokines to the normal brain, it is not well known to what extent the BBB is patent or compromised in developing brain metastases; to the extent that the BBB is patent, this would also contribute to an altered environment. Based on these observations, we hypothesized that brain metastases would exhibit distinct gene expression trends. A microarray analysis of gene expression was conducted using flash-frozen samples of resected brain metastases of breast cancer. It would be impossible to identify frozen matched primary tissues for these brain metastases; therefore, unlinked primary breast tumors matched for hormone receptor and tumor-node-metastasis status were used for comparison. While using imperfect matches, and limited in the number of

Table 3. Cox Proportional Hazards Model Analysis of Patient Survival after Resection for Brain Metastasis of Breast Cancer

Variable	HR (95% CI)	*P*
Her-2	0.50 (0.31-0.83)	0.0065
ER	0.41 (0.24-0.71)	0.0015
HK2	2.52 (1.27-4.97)	0.0080

NOTE: Based on staining results from 113 patients with complete data on the three parameters.
Abbreviations: HR, hazard ratio; CI, confidence interval.

specimens available, the potential insights afforded by actual clinical material as opposed to cell lines is inarguable. Another advantage of the experimental design was that epithelial cells were purified by LCM from each lesion, so that gene expression differences due to contaminating nontumor cells in the surgical margin were not present. The microarray analysis indicated that brain metastases differentially express several genes by 2- to 3-fold, including phosphatases, glycosylphosphatidylinositol-anchoring proteins, and those regulating the extracellular matrix and cell adhesion. Differential gene expression was validated using a semi-independent set of brain metastases and primary tumors, the experimental design again dependent on availability of craniotomy specimens suitable for molecular analysis. Statistically significant differences or trends ($P < 0.1$) in differential gene expression were observed for six genes. Given the limited sample size, our conclusion is that all of these trends may be of biological importance. Several of these genes are under further investigation. Recently, Bos et al. reported 243 genes that were differentially expressed between brain metastatic and primary cell lines. From this data set, two genes overlap with our findings in the surgical specimens. *CASK* (calcium/calmodulin-dependent serine protein kinase) was up-regulated in the brain metastatic cohorts, whereas *TRIM34* (tripartite motif-containing 34) was down-regulated (31).

HK2 was a compelling target for several reasons, including its reported involvement in bioenergetics and apoptosis. Hexokinase expression and activity is up-regulated in breast cancer compared with normal breast tissue (32), and limited data suggested that it is further up-regulated in metastases (33). In addition, HK2 was one of few genes up-regulated in the brain metastases, so that inhibitors with potential therapeutic benefit could be considered.

Using the 231-BR model system, HK expression was down-regulated ~2-fold using two different shRNAs. Under normal tissue culture conditions, no difference was observed between the control and HK2 shRNA clones in ATP levels/viability or drug-induced apoptosis. However, normal serum glucose levels are 7 to 10 mg/L, in contrast to a concentration of 4.5 g/L in normal cell culture medium. Therefore, the experiments were repeated using 10% of the standard glucose concentration, conditions in which we expect that metabolism of glucose by the cells decreases the glucose concentration to physiologic levels over the time course of the experiment. Under these conditions, the HK2 knockdown cells exhibited altered growth kinetics. Viability, as assessed by both intracellular ATP concentrations and MTT assay, was reduced in the HK2 knockdowns. A reduction in proliferation by down-regulation of HK2 was also reported for LoVo colon cancer cells (34). Circumstantial evidence suggests that conditions of limited nutrient availability may exist in brain metastases. Necrotic centers were observed in at least 8 of 16 resected human brain metastases, indicative of poor vascularization (26). The data therefore suggest a functional role for altered HK2 expression in cell growth under conditions of limited nutrient availability. This difference will be difficult to confirm *in vivo*. The 231-BR model produces multiple brain metastases after intracardiac injection, but mice must be routinely sacrificed 1 month after injection according to Animal Care and Use Committee guidelines due to neurologic deficits (paralysis) and weight loss, a point too early for the formation of large necrotic metastases (23, 26, 35). To overcome this, new models of breast cancer brain metastasis will be needed that recapitulate necrosis and conditions of nutrient availability.

No difference in apoptosis induced by drugs or radiation was observed between the control and HK2 knockdown clones (data not shown). These data may reflect the recent discovery that glucose metabolism can exert other functions to regulate apoptosis, such as the oxidation of cytochrome *c* (36). Thus, glucose metabolism pathways downstream of HK2 interaction with the mitochondrion may alter its effects on apoptosis. It is also possible that HK1 could compensate for the reduced expression of HK2 in the apoptotic pathway, as HK1 is capable of binding to mitochondria.

The potential significance of HK2 overexpression in brain metastases of breast cancer was confirmed by an immunohistochemical analysis in a cohort of craniotomy specimens. Approximately 77% of the craniotomy specimens exhibited high HK2 expression, and this was associated with reduced survival after resection ($P = 0.028$). These data may not apply to all brain metastases, as patients with a limited number of brain lesions that are located in accessible regions of the brain are typical surgical candidates. If validated, therapeutic approaches to inhibit HK2 may be considered. Although this enzyme is ubiquitous and instrumental for cell function, a reduction in its activity rather than a complete elimination may be an achievable target. Several compounds have been identified against the potential antiapoptotic role for HK2 (19, 37-39) but would be of limited benefit in the 231-BR model system. Other agents directed at the bioenergetic activity of HK2, if BBB permeable, would be of high interest.

Materials and Methods

Specimens

Frozen brain metastases were collected from Vanderbilt University, the University of Schleswig-Holstein Medical Center, and the NIH. Frozen primary invasive breast samples were collected from the University of Schleswig-Holstein Medical Center or University of Tuebingen. All samples were anonymized and approved by the National Cancer Institute Office of Human Subjects Research. Diagnosis and histopathologic characteristics were confirmed by a single pathologist before use in the study.

Expression Profiling of Tumor Cohorts

All samples were subjected to LCM and RNA amplification. Briefly, 8-μm frozen tissue sections were thawed 15 s at room temperature and stained using Histogene LCM Frozen Section Staining kit (Arcturus Engineering) following the manufacturer's instructions with the addition of a 5-min incubation in 100% ethanol before xylene. Approximately 2,000 laser-captured pulses were collected for each sample using the PixCell II Laser Capture Microdissection System (Arcturus Engineering) in a 15-min period. Captured cells were lysed off the LCM caps in PicoPure RNA Extraction buffer (PicoPure RNA Isolation kit, Arcturus Engineering) for 30 min at 55°C and frozen at −80°C until ready to proceed. Total RNA was extracted according to the manufacturer's instructions for the PicoPure RNA Isolation kit. Quality and quantity of

RNA were assessed using the RNA 6000 Pico Assay for the 2100 Bioanalyzer (Agilent Technologies). A minimum of 10 ng of RNA was then subjected to two rounds of a T7 RNA polymerase catalyzed amplification protocol using the RiboAmp RNA Amplification kit (Arcturus Engineering). Quality and quantity of the amplified aRNA were assessed using the RNA 6000 Nano Assay for the 2100 Bioanalyzer. A reference RNA sample consisting of a pool of six breast cancer cell lines (MCF7, ZR-75, BT-474, BT-549, MDA-MB-231, and T-47-D) was simultaneously amplified.

cDNA microarray analysis: Cy3-dUTP–labeled or Cy5-dUTP–labeled cDNA (GE Healthcare) was synthesized from 50 to 100 μg of amplified aRNA using random primed polymerization with SuperScript II reverse transcriptase (Invitrogen). Equal amounts of labeled cDNA for the test sample and the reference sample were hybridized to cDNA array for each tumor. Arrays were constructed on glass slides from PCR products representing the inserts of 28,411 IMAGE consortium cDNA clones in the National Human Genome Research Institute microarray core laboratory. Fluorescent intensities were measured using an Agilent scanner, and scanned images were analyzed using DeArray software. Significance of microarray analysis was used for data mining and analysis. Supervised clustering was done, where each sample was identified as brain metastasis or primary tumor and the ER or Her-2 status was identified.

Quantitative Real-time PCR

Double-stranded cDNA was prepared using the second-round synthesis protocol from the RiboAmp RNA amplification kit. Q-PCRs consisted of 1× SYBR Green Supermix (Bio-Rad Laboratories), 0.2 mmol/L of forward and reverse primers, and 10 ng cDNA. Cycling conditions consisted of three-step amplification and melt curve analysis using the iQ5 Real-Time PCR Detection System (Bio-Rad Laboratories). For generating a standard curve, amplified cDNA from the reference sample detailed above was used in a 5-fold dilution series. Relative gene expression was calculated by dividing the specific expression value (starting quantity, ng) by the glyceraldehyde-3-phosphate dehydrogenase expression value.

Cell Culture and Knockdown of HK2 with shRNA

A brain metastatic derivative of the breast cancer cell line MDA-MB-231 was isolated and described previously (24). These cells, designated 231-BR, were maintained in high-glucose DMEM (Invitrogen) and supplemented with 10% fetal bovine serum (Invitrogen) and penicillin-streptomycin (Invitrogen) at 37°C in 5% CO_2. Clones of 231-BR cells with stable knockdown of HK2 expression were generated using a commercial lentiviral system for introduction of shRNAs (Sigma). Sigma Mission Non-Target shRNA (SHC002V) was used to generate control cell lines, and two shRNAs, TRCN 0000037669 and TRCN 0000037673, were used for knockdown of HK2 expression. Lentiviral particles (2×10^5) were added to 231-BR cells for 24 h, and cells were subsequently cultured in medium containing 1 μg/mL puromycin. Cells were maintained and expanded in this selective medium to select individual clones with stable knockdown.

Western Blot Analysis

Western blots were done using standard protocols. Briefly, 231-BR cell lysates were prepared in radioimmunoprecipitation assay buffer [20 mmol/L Tris-HCl (pH 8), 100 mmol/L NaCl, 10% glycerol, 1% NP40, 0.5% sodium deoxycholate, 0.1% SDS] supplemented with a Complete Mini protease inhibitor cocktail (Roche). Protein lysates (50-100 μg) were separated using SDS-PAGE. Proteins were transferred to nitrocellulose and blots were incubated for 2 h to overnight with the following antibodies: rabbit anti-HK1 polyclonal antibody (1:2,000 dilution; Millipore), rabbit anti-HK2 polyclonal antibody (1:5,000 dilution; Millipore), rabbit anti-HK2 polyclonal antibody (1:500 dilution; Abgent), rabbit anti-HK3 polyclonal antibody (1:500 dilution; Abgent), and rabbit anti-glucokinase (HK4; 1:200 dilution; Santa Cruz Biotechnology). Goat anti-rabbit horseradish peroxidase (1:5,000; Santa Cruz Biotechnology) was used as a secondary antibody. Enhanced chemiluminescence was used for detection.

Cell Viability Assay

Cells were seeded in normal growth medium (high-glucose DMEM, 10% fetal bovine serum with no additional additives). This medium was diluted 1:10 with glucose-free DMEM for glucose-limiting experiments, and viability was measured at various time points. The CellTiter-Glo Luminescent Cell Viability Assay (Promega) was used to measure cellular ATP levels. This assay was conducted in 96-well opaque-walled luminescence plates (Perkin-Elmer), and relative ATP levels were measured using a luminometer (Promega GloMax). Replicate 96-well plates were prepared, and each sample was analyzed in quadruplicate wells.

Immunohistochemistry

Archival paraffin-embedded tumor samples were obtained at the M. D. Anderson Cancer Center from patients with a history of breast cancer who presented with metastases to the central nervous system parenchyma. The median age of the cohort was 51 y, with a range from 27 to 75 y. Thirty-three of 124 patients (26.6%) had ER-positive brain metastasis, and 45 of 124 (36.2%) had Her-2 amplification. Sections from these samples were confirmed to have metastatic breast cancer present and subjected to immunohistochemistry for HK2. Sections were processed and stained as previously described (40) using an anti-HK2 antibody (Millipore) at a 1:500 dilution with microwave antigen retrieval in 10 mmol/L sodium citrate buffer. Scoring was done using a three-tiered system (no, low, or high) for HK2 protein levels.

Statistical Analysis

Survival of patients was determined from date of craniotomy until date of death or date of last follow-up as appropriate. The probability of survival as a function of time was determined by the Kaplan-Meier method, and the statistical significance of the difference between two Kaplan-Meier curves was determined by a two-tailed log-rank test. A Cox proportional hazards model was used to determine the statistical significance of HK2 on survival when evaluated along with ER and Her-2 status. A likelihood ratio test was used to determine the statistical significance of HK2 when this parameter was added to a model that had consisted of ER and Her-2

status, and provides the additional effect of this parameter when added to the model. A one-way ANOVA was done on the average results from control clones and three HK2 knockdown clones, from $n = 3$ experiments, for the *in vitro* data in Fig. 3. The results were adjusted using Holm's method. Comparisons of expression levels of genes were done using an exact Wilcoxon rank sum test. In view of the number of tests done, only P values of ≤ 0.01 should be interpreted as being statistically significant, whereas those for which $0.01 < P < 0.05$ would be considered strong trends.

Disclosure of Potential Conflicts of Interest

No potential conflicts of interest were disclosed.

Acknowledgments

We thank Dr. Abdel Elkahloun for construction of the cDNA microarrays used herein.

References

1. Lin N, Bellon J, Winer E. CNS metastases in breast cancer. J Clin Oncol 2004; 22:3608–17.

2. Weil R, Palmieri D, Bronder J, Stark A, Steeg P. Breast cancer metastasis to the central nervous system. Am J Pathol 2005;167:913–20.

3. Lin NU, Winer EP. Brain metastases: the HER2 paradigm. Clin Cancer Res 2007;13:1648–55.

4. Evans A, James J, Cornford E, et al. Brain metastases from breast cancer: identification of a high-risk group. Clin Oncol (R Coll Radiol) 2004;16:345–9.

5. Smid M, Wang Y, Zhang Y, et al. Subtypes of breast cancer show preferential site of relapse. Cancer Res 2008;68:3108–14.

6. Slimane K, Andre F, Delaloge S, et al. Risk factors for brain relapse in patients with metastatic breast cancer. Ann Oncol 2004;15:1640–4.

7. Pestalozzi BC, Zahrieh D, Price KN, et al. Identifying breast cancer patients at risk for central nervous system (CNS) metastases in trials of the International Breast Cancer Study Group (IBCSG). Ann Oncol 2006;17:935–44.

8. Carey LA, Ewend MG, Metzger R, et al. Central nervous system metastases in women after multimodality therapy for high risk breast cancer. Breast Cancer Res Treat 2004;88:273–80.

9. Ryberg M, Nielsen D, Osterlind K, Andersen PK, Skovsgaard T, Dombernowsky P. Predictors of central nervous system metastasis in patients with metastatic breast cancer. A competing risk analysis of 579 patients treated with epirubicin-based chemotherapy. Breast Cancer Res Treat 2005;91:217–25.

10. Tham YL, Sexton K, Kramer R, Hilsenbeck S, Elledge R. Primary breast cancer phenotypes associated with propensity for central nervous system metastases. Cancer 2006;107:696–704.

11. Hicks D, Short S, Prescott N, et al. Breast cancers with brain metastases are more likely to be estrogen receptor negative, express the basal cytokeratin CK5/6 and over-express Her-2 or EGFR. Am J Surg Pathol 2006;30:1097–104.

12. Peng SY, Lai PL, Pan HW, Hsiao LP, Hsu HC. Aberrant expression of the glycolytic enzymes aldolase B and type II hexokinase in hepatocellular carcinoma are predictive markers for advanced stage, early recurrence and poor prognosis. Oncol Rep 2008;19:1045–53.

13. Lyshchik A, Higashi T, Hara T, et al. Expression of glucose transporter-1, hexokinase-II, proliferating cell nuclear antigen and survival of patients with pancreatic cancer. Cancer Invest 2007;25:154–62.

14. Rho M, Kim J, Jee CD, et al. Expression of type 2 hexokinase and mitochondria-related genes in gastric carcinoma tissues and cell lines. Anticancer Res 2007;27: 251–8.

15. Smith TA. Mammalian hexokinases and their abnormal expression in cancer. Br J Biomed Sci 2000;57:170–8.

16. Pedersen PL. Voltage dependent anion channels (VDACs): a brief introduction with a focus on the outer mitochondrial compartment's roles together with hexokinase-2 in the "Warburg effect" in cancer. J Bioenerg Biomembr 2008.

17. Galluzzi L, Kepp O, Tajeddine N, Kroemer G. Disruption of the hexokinase-VDAC complex for tumor therapy. Oncogene 2008;27:4633–5.

18. Robey RB, Hay N. Mitochondrial hexokinases, novel mediators of the anti-apoptotic effects of growth factors and Akt. Oncogene 2006;25:4683–96.

19. Machida K, Ohta Y, Osada H. Suppression of apoptosis by cyclophilin D via stabilization of hexokinase II mitochondrial binding in cancer cells. J Biol Chem 2006;281:14314–20.

20. Pastorino JG, Hoek JB. Regulation of hexokinase binding to VDAC. J Bioenerg Biomembr 2008.

21. Paudyal B, Oriuchi N, Paudyal P, Higuchi T, Nakajima T, Endo K. Expression of glucose transporters and hexokinase II in cholangiocellular carcinoma compared using [^{18}F]-2-fluro-2-deoxy-D-glucose positron emission tomography. Cancer Sci 2008;99:260–6.

22. Yamada K, Brink I, Bisse E, Epting T, Engelhardt R. Factors influencing [F-18] 2-fluoro-2-deoxy-D-glucose (F-18 FDG) uptake in melanoma cells: the role of proliferation rate, viability, glucose transporter expression and hexokinase activity. J Dermatol 2005;32:316–34.

23. Palmieri D, Bronder JL, Herring JM, et al. Her-2 overexpression increases the metastatic outgrowth of breast cancer cells in the brain. Cancer Res 2007;67: 4190–8.

24. Yoneda T, Williams P, Hiraga T, Niewolna M, Nishimura R. A bone seeking clone exhibits different biological properties from the MDA-MB-231 parental human breast cancer cells and a brain-seeking clone *in vivo* and *in vitro*. J Bone Miner Res 2001;16:1486–95.

25. Bendell J, Domchek S, Burstein H, et al. Central nervous system metastases in women who receive trastuzumab-based therapy for metastatic breast carcinoma. Cancer 2003;97:2972–7.

26. Fitzgerald D, Palmieri D, Hua E, et al. Reactive glia are recruited by highly proliferative brain metastases of breast cancer and promote tumor cell colonization. Clin Exp Metastasis 2008;25:799–810.

27. Marchetti D, Li J, Shen R. Astrocytes contribute to the brain-metastatic specificity of melanoma cells by producing heparanase. Cancer Res 2000;60: 4767–70.

28. Sierra A, Price J, Garcia-Ramirez M, Mendez O, Lopez L, Fabra A. Astrocyte derived cytokines contribute to the metastatic brain specificity of breast cancer cells. Lab Invest 1997;77:357–68.

29. Zhang M, Olsson Y. Reactions of astrocytes and microglial cells around hematogenous metastases of the human brain. Expression of endothelin-like immunoreactivity in reactive astrocytes and action of microglial cells. J Neurol Sci 1995;134:26–32.

30. Deeken JF, Loscher W. The blood-brain barrier and cancer: transporters, treatment, and Trojan horses. Clin Cancer Res 2007;13:1663–74.

31. Bos P, Zhang X, Nadal C, et al. Genes that mediate breast cancer metastasis to the brain. Nature 2009;459:1005–9.

32. Balinsky D, Platz C, Lewis J. Enzyme activities in normal, dysplastic and cancerous human breast tissues. J Natl Cancer Inst 1984;72:217–24.

33. Hennipman A, Oirschot BV, Smits J, Rijksen G, Staal G. Glycolytic enzyme activities in breast cancer metastases. Tumour Biol 1988;9:241–8.

34. Peng Q, Zhou Q, Zhong J, Pan F, Liang H. Stable RNA interference of hexokinase II gene inhibits human colon cancer LoVo cell growth *in vitro* and *in vivo*. Cancer Biol Ther 2008;7:1128–35.

35. Gril B, Palmieri D, Bronder JL, et al. Effect of lapatinib on the outgrowth of metastatic breast cancer cells to the brain. J Natl Cancer Inst 2008;100:1092–103.

36. Vaughn A, Deshmukh M. Glucose metabolism inhibits apoptosis in neurons and cancer cells by redox inactivation of cytochrome *c*. Nat Cell Biol 2008;10: 1477–85.

37. Penso J, Beitner R. Lithium detaches hexokinase from mitochondria and inhibits proliferation of B16 melanoma cells. Mol Genet Metab 2003;78:74–8.

38. Penso J, Beitner R. Clotrimazole decreases glycolysis and the viability of lung carcinoma and colon adenocarcinoma cells. Eur J Pharmacol 2002;451: 227–35.

39. Goldin N, Heyfets LAA, Israelson A, et al. Methyl jasmonate binds to and detaches mitochondria-bound hexokinase. Oncogene 2008;27:4636–43.

40. Simmons ML, Lamborn KR, Takahashi M, et al. Analysis of complex relationships between age, p53, epidermal growth factor receptor, and survival in glioblastoma patients. Cancer Res 2001;61:1122–8.